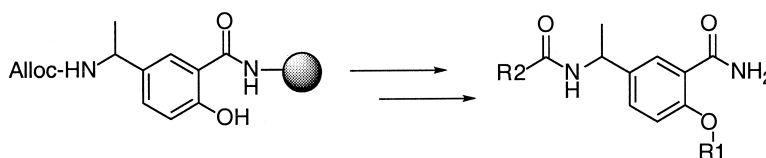Article

Structure-Based Design and Solid-Phase Parallel Synthesis of Phosphorylated Nonpeptides to Explore Hydrophobic Binding at the Src SH2 Domain

Chester A. Metcalf, Charles J. Eyermann, Regine S. Bohacek, Chad A. Haraldson, Vaibhav M. Varkhedkar, Berkley A. Lynch, Catherine Bartlett, Shelia M. Violette, and Tomi K. Sawyer

More About This Article

Additional resources and features associated with this article are available within the HTML version:

- Supporting Information
- Access to high resolution figures
- Links to articles and content related to this article
- Copyright permission to reproduce figures and/or text from this article

View the Full Text HTML

Articles

Structure-Based Design and Solid-Phase Parallel Synthesis of Phosphorylated Nonpeptides to Explore Hydrophobic Binding at the Src SH2 Domain

Chester A. Metcalf III,* Charles J. Eyermann, Regine S. Bohacek, Chad A. Haraldson, Vaibhav M. Varkhedkar, Berkley A. Lynch, Catherine Bartlett, Shelia M. Violette, and Tomi K. Sawyer

ARIAD Pharmaceuticals, Inc., 26 Landsdowne Street, Cambridge, Massachusetts 02139-4234

Using a novel, solid-phase parallel synthetic route and a computational docking program, a series of phosphorylated nonpeptides were generated to determine their structure−activity relationships (SAR) for binding at the SH2 domain of pp60src (Src). A functionalized benzoic acid intermediate was attached to solid support via Rink amide linkage, which upon acid cleavage generated the desired benzamide template-based nonpeptides in a facile manner. Compounds were synthesized using a combination of solid- and solution-phase techniques. Purification using reversed-phase, semipreparative HPLC allowed for quantitative SAR studies. Specifically, this work focused on functional group modifications, in a parallel fashion, designed to explore hydrophobic binding at the pY+3 pocket of the Src SH2 domain.

Introduction

The discovery of lead compounds, via high-throughput screening, for a variety of biological targets has been accelerated through the utilization of combinatorial libraries;[1] traditionally these compound collections have been synthesized as mixtures. Techniques involving parallel solid-phase synthesis provide rapid access to multiple, discrete analogues and allow SAR interpretation at both lead generation and lead optimization stages. To broaden the synthetic scope of this field, a reaction scheme combining both solid- and solution-phase reactions can be followed to provide compounds of varying complexity and diversity. This approach recognizes the strengths and limitations of each synthetic methodology and then devises a route accordingly, maximizing yield and purity.[2] Furthermore, structure-based drug design may be integrated with combinatorial chemistry to facilitate and enhance the iterative optimization cycles of drug discovery for a specific biological target.[3]

A variety of proteins involved in signal transduction contain noncatalytic Src homology-2 (SH2) domains that function as mediators of intracellular protein−protein interactions. These SH2 domains (∼100 amino acids in size) bind pTyr-containing proteins and peptides in a sequence depend-
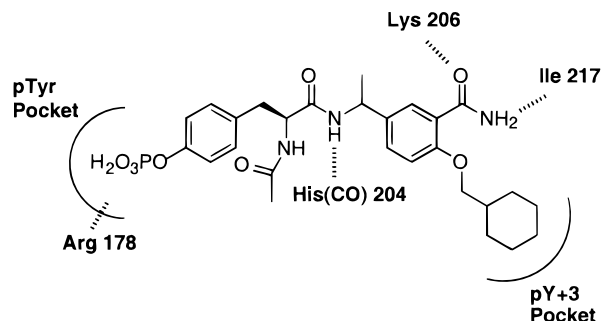

Figure 1. Binding interactions of compound **1a** with Src SH2.

ent manner,[4] which provides on a cellular level the basis for differentiation of the phosphorylation/dephosphorylation events surrounding a multitude of signaling pathways.[5,6] This intricate role of SH2 domains in cell function coupled with the postulated involvement of the nonreceptor tyrosine kinase Src in various disease states (i.e., cancer, osteoporosis)[7] provides an impetus to develop Src SH2-binding small molecules as therapeutic modulators of the aberrant signaling activity associated with these diseases.[8,9] The major binding regions of Src SH2 as determined by X-ray crystallography[10,11] are the pTyr and pY+3 (pTyr+3) pockets (Figure 1). The pY+3 region of Src SH2 is highly hydrophobic in nature, characterized by Tyr 205, Ile 217, and Leu 240 residues, with additional H-bonding possibilities from Tyr 205, Thr 218, as well as a buried Tyr 233 protein residue. Much of our understanding of Src SH2−ligand interactions

* Address correspondence to Chester A. Metcalf III, Ph.D., Staff Scientist, ARIAD Pharmaceuticals, Inc., 26 Landsdowne Street, Cambridge, MA 02139-4234. E-mail: chet.metcalf@ariad.com. Phone: (617) 494-0400 x244. Fax: (617) 494-8144.
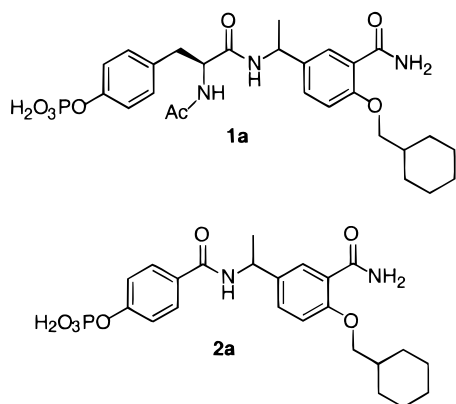
Figure 2. Src SH2 nonpeptide compounds **1a** and **2a**.

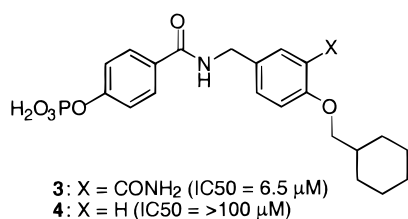**3**: X = CONH₂ (IC50 = 6.5 µM)
4: X = H (IC50 = >100 µM)

Figure 3. Effect of carboxamide group on Src SH2 binding affinity.

comes from complexed protein structures with peptides containing the high-affinity motif pTyr-Glu-Glu-Ile, a sequence preferred by Src SH2 as first shown in an elegant study by Cantley et al. in 1993.[4] Some significant protein−ligand interactions include Arg 178 with the phosphate oxygens of pTyr, mutation of which abolishes all binding,[12] and a direct H-bonding contact involving the ligand pY+1 Glu backbone NH and the carbonyl oxygen of the His 204 protein residue.

We were interested in probing the pY+3 interactions of a high-affinity nonpeptide, **1a**[13a] (Figure 2), at the SH2 domain of Src, as part of an ongoing effort to develop novel inhibitors of Src SH2-associated signal transduction pathways.[14] Although there are a number of papers describing the interactions of peptides/peptidomimetics with Src family and related SH2 domains,[13] the pY+3 region of Src SH2 domain has been explored only on a limited basis with nonpeptidic small molecule inhibitors.[15,16] Also, observations from our modeling studies as well as others[15] suggest that a cyclohexyl group does not allow for the most optimal pY+3 interactions, as it primarily engages only surface type contacts with the protein.

In this report, we describe an integrated strategy that utilizes the rapid analogue generation capabilities of parallel synthesis to understand the binding possibilities available to derivatives of compound **1** through structurally biased modifications made to the pY+3 site of the molecule.[17] For our study, a combination of both solid- and solution-phase reactions were employed to generate the required compounds for quantitative SAR evaluation. A computational docking program was used to identify appropriate pY+3 substituents. In addition, compounds related to structure **2a**[16] (Figure 2) were generated to demonstrate the versatility of the solid-phase synthetic method.

Scheme 1[a]
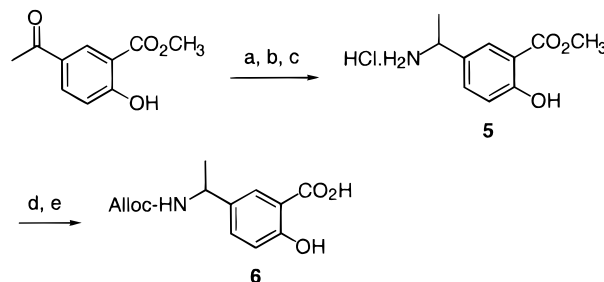
[a] Reagents and conditions: (a) HONH₂·HCl, pyridine, rt, 22 h; (b) Raney Ni, 45 psi H₂ (Parr apparatus), EtOH/Et₃N (5:1); (c) HCl·Et₂O; (d) 2.3 N NaOH, DME; (e) diallyl dicarbonate/DME.

Results

Solid-Phase Chemistry Strategy and Synthesis. Modeling studies as well as an X-ray crystal structure[17] demonstrate that the carboxamide functionality contained in the benzamide template of **1a** is critical for binding, interacting with both the Lys 206 and the Ile 217 protein residues of Src SH2 (Figure 1). The effect on Src SH2 binding can be seen in a reported result[16] for the related compounds **3** and **4** (Figure 3), in which the des-amide compound **4** shows a greater than 15-fold decrease in binding affinity compared to the parent compound **3**. The benzamide structural information coupled with the attractiveness of parallel synthesis for rapid compound generation prompted us to devise a hitherto unreported solid-phase route to compounds **1a** and **2a** along with their pY+3 derivatives, exploiting the carboxamide functionality in a dual capacity role as both a linker attachment site and conserved binding element. The selection of a Rink amide linker was made based on straightforward template attachment and eventual generation of the critical binding moiety upon cleavage. It was decided at an early stage, taking into consideration overall yield and chemistry efficiency, to construct the central salicylic template separately in bulk using solution-phase techniques. Modification of the literature procedure[18] allowed construction of the template with the necessary functionality for attachment to the solid support and subsequent analogue generation. This synthetic strategy still realizes the full benefits of parallel synthesis, since the diversity elements are introduced after the template-containing resin has been loaded into the parallel synthesizer. The number of nondiversity solid-phase steps requiring reaction optimization are also minimized using this protocol. Thus, preparation of **6** started with condensation of commercially available methyl 5-acetylsalicylate with hydroxylamine hydrochloride (Scheme 1). Hydrogenation with Raney nickel in a Parr apparatus (45 psi) and precipitation with a 1.0 M solution of Et₂O·HCl provided clean amine hydrochloride **5**. One-pot hydrolysis and Alloc protection followed by workup and recrystallization from EtOAc/CH₂Cl₂ provided the salicylic acid template **6** in excellent yield and purity for subsequent resin attachment.[19]

Template **6** was coupled to Rink amide AM resin (Novabiochem) in batch using standard protocols (EDC/HOBt) to provide, upon excess solvent removal, resin **7** with an assumed theoretical loading capacity of 0.65 mmol/g (Scheme 2). The charged resin **7** was loaded into pre-silylated reaction vessels (RVs) and placed into a Nautilus 2400 organic syn-

Scheme 2[a]
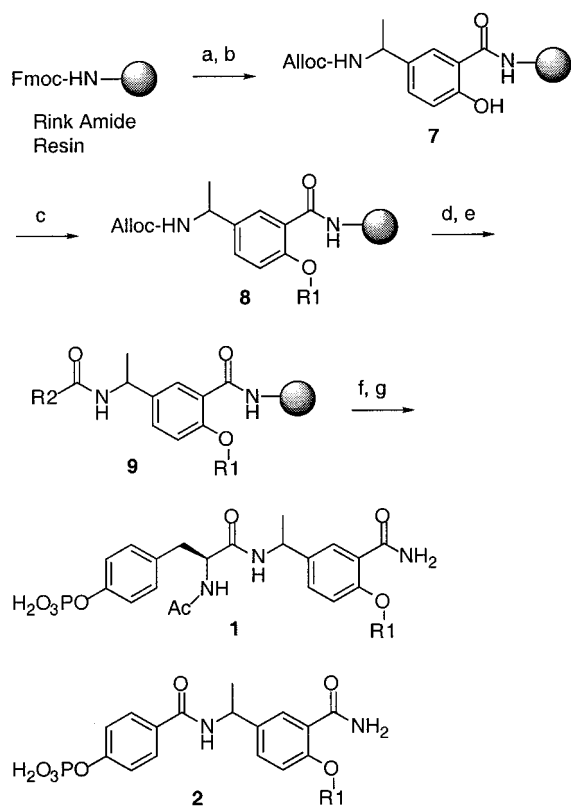
[a] Reagents and conditions: (a) 20% piperidine/DMA; (b) **6**, EDC, HOBt, DCM/DMA (3:1); (c) DEAD, Ph₃P, R1-OH, THF, rt (double coupling); (d) Pd(Ph₃P)₄, Ph₃P, HOBt, DCM/DMF (2:1); (e) R2-CO₂H, EDC, HOBt, DIEA, DCM/DMA (3:1), 0 °C−rt; (f) 95% TFA/2.5% H₂O/2.5% TIS, 1−2 h; (g) RP-HPLC purification.

thesizer[20] where analogue generation took place. Mitsunobu coupling using the diversity alcohols R1-OH under double coupling conditions generated the resin-bound ether **8**. Sterically hindered and electron-poor alcohols (e.g., 2,4-dimethyl-3-pentanol and 1,1,1,3,3,3-hexafluoro-2-propanol) failed to provide coupled product. Alloc deprotection and amide formation with either Ac-Tyr(PO₃Bn₂)-OH[21] or p-(OPO₃Bn₂)PhCO₂H[21] using an EDC/HOBt activation procedure provided the coupled resin product **9** with each individual RV containing a discrete product. At each step throughout the solid-phase reaction sequence, representative resin aliquots (ca. 3 mg/ea) from several of the RVs were cleaved and analyzed by HPLC and LRMS (ES±) to verify product formation. A typical analytical protocol involved the addition of 5−30% TFA in dichloromethane to a 1 dram vial containing the resin and then allowing ∼5 min to lapse before concentrating the sample with a stream of N₂. This was repeated with 100% dichloromethane followed by the addition of 0.4 mL of 50:50 acetonitrile/water (1 drop of DMSO pre-added to dissolve the sample), filtration by centrifuge (0.45 μm filter inserts), and analysis of the divided filtrates. This method was mild enough not to jeopardize the integrity of the intermediate products, while providing in a timely fashion (similar to taking a TLC) ample amounts of cleavage material for reaction assessment. Benzyl phosphate deprotection and concurrent resin cleavage with 95% TFA/H₂O followed by concentration of the cleavage solutions provided the crude product residues. The resulting oils/

semisolids were then purified by reversed-phase (RP) semi-preparative HPLC to provide the products **1a−h** and **2a,d,f,g**. Overall yields of the purified products are provided in Table 1 and ranged from 23 to 76% (50% av). No attempts were made during HPLC purification to separate the diastereomeric peaks of **1a−h**, and in all cases the approximately 50/50 mixture (verified by ¹H NMR) of diastereomeric products were assayed as such.
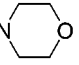
Assay. Compounds were tested for binding to Src SH2 using a fluorescence polarization (FP) binding assay according to methods previously described.[22,14a] IC₅₀ values were assigned to individual compounds according to their competitive binding affinity versus a high-affinity peptide probe, fluorescein-pTyr-pTyr-pTyr-Ile-Glu-NH₂.

Computational Method for Selection of pY+3 Groups. The diversity chemistry allows the addition of almost any primary or secondary alcohol to the benzamide template; therefore, molecular modeling was used to aid in the selection of those side chains predicted to form the most favorable interactions with the pY+3 binding site atoms. Commercially available alcohols were selected for a virtual screening study using a molecular weight cutoff of less than 250 Da (larger groups would not sterically fit into the pY+3 site). Furthermore, chemistry filters which did not allow additional H-bond donors beyond the alcohol group were utilized. Functional groups such as metals, isotopes, and reactive centers other than the hydroxyl group were eliminated as well. The resulting 800 alcohols were converted to 3D using CONCORD. Each alcohol was then attached to the benzamide scaffold of **1**, using the new combinatorial module of FLO,[23] and docked into the Src SH2 binding site model (described below). Each docking was then scored based on the protein−ligand hydrophobic and H-bond interaction energies, as well as internal ligand strain energy. The highest scoring alcohols were visually reviewed and those of interest more rigorously docked and minimized.
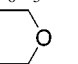
The Src SH2 binding site model used in this study was developed based on a high resolution (1.0 Å) crystal structure of Lck SH2 complexed with Ac-pTyr-Glu-Glu-Ile-NH₂, obtained from the Brookhaven Protein Data Bank (reference 1LKK).[24] Docking was carried out using the MCDOCK conformational searching/energy minimization procedure of FLO.[25] This program uses extensive conformational searching and energy minimization to identify the conformation a molecule is likely to adopt upon binding to SH2. During the docking procedure, most binding site atoms are held fixed. However, those residues known to change conformation upon binding with different ligands are allowed to move freely during the energy minimization step. Binding site atoms displaying smaller changes in position are constrained with a force constant. Docked molecules were evaluated using the following energies and scoring values reported by FLO: internal ligand energy (the energy of the docked conformation calculated without the binding site corrected for ligand global minimum energy), contact energy (an energy term representing contacts between ligand and binding site atoms), H-bonding score (the number of contacts between ligand H-bonding atoms and complementary areas of the binding site accessible surface), and hydrophobic contact

Table 1. Product Data for Generated Compounds

compd no.	R1	formula	MW	% yield[a] (final product)
1a	$CH_2C_6H_{11}$	$C_{27}H_{36}N_3O_8P$	561.58	43
1b	CH_3	$C_{21}H_{26}N_3O_8P$	479.43	47[b]
1c	CH_2CH_3	$C_{22}H_{28}N_3O_8P$	493.46	70
1d	$CH(CH_3)_2$	$C_{23}H_{30}N_3O_8P$	507.48	76
1e	C_6H_{11}	$C_{26}H_{34}N_3O_8P$	547.55	58
1f	$CH(CH_2CH{=}CH_2)_2$	$C_{27}H_{34}N_3O_8P$	559.56	32
1g	$CH_2CH_2CH_2C_6H_5$	$C_{29}H_{34}N_3O_8P$	583.58	59
1h	$CH_2CH_2{-}N$⬡O	$C_{26}H_{35}N_4O_9P{\cdot}TFA$	692.59	62
2a	$CH_2C_6H_{11}$	$C_{23}H_{29}N_2O_7P$	476.47	39
2d	$CH(CH_3)_2$	$C_{19}H_{23}N_2O_7P$	422.37	50
2f	$CH(CH_2CH{=}CH_2)_2$	$C_{23}H_{27}N_2O_7P$	474.45	23
2g	$CH_2CH_2CH_2C_6H_5$	$C_{25}H_{27}N_2O_7P$	498.47	39

[a] Yields were based on an assumed theoretical loading capacity of 0.65 mmol/g for **7** and refer to final HPLC purified and lyophilized products. [b] A total of 16% of monobenzyl phosphate product was also isolated following purification as a consequence of incomplete benzyl phosphate deprotection.

Table 2. FP Binding Data for Compounds **1a−1h**

compd no.	R1	Src SH2 FP binding (IC_{50}, μM)	rel. potency (IC_{50} **1a**/ IC_{50} compd)
1a	$CH_2C_6H_{11}$	1.9	1.0
1b	CH_3	37	0.05
1c	CH_2CH_3	27	0.07
1d	$CH(CH_3)_2$	7.5	0.25
1e	C_6H_{11}	2.6	0.7
1f	$CH(CH_2CH{=}CH_2)_2$	0.9	2.1
1g	$CH_2CH_2CH_2C_6H_5$	6.5	0.29
1h	$CH_2CH_2{-}N$⬡O	335	0.006

score (the number of contacts between hydrophobic ligand atoms and hydrophobic areas of the binding site accessible surface).

Discussion

Relative to compound **1**, the selection of R1 (pY+3) groups for this study was based on both their predicted binding to Src SH2 and ability to impart beneficial properties to the molecule as a whole (i.e., reduced MW, increased solubility, etc.). The input for R1 group selection was based on the aforementioned FLO program as well as established drug design principles. Table 2 lists the Src SH2 FP binding affinities for compounds **1a−h**. Compound **1a** was synthesized using our solid-phase method to act as an internal standard for our generated analogues.[26]

The methyl analogue **1b** binds with less affinity compared to **1a** (20-fold), which is expected based on the number of hydrophobic contacts each can make. An increase in affinity is observed with increased hydrophobicity as seen in compound **1c** (ethyl) and also in **1d** (isopropyl), which has a 5-fold greater affinity than **1b**. In addition, compound **1d** exhibits approximately 4-fold lower affinity than **1a**. This result is significant, from a drug design perspective, since a four-carbon reduction (MW loss of 54) was achieved without greatly compromising the binding affinity of the compound. A one-carbon-atom truncation of the cyclohexylmethyl group of compound **1a** does not appear to greatly affect binding as demonstrated by compound **1e**. However, compounds **1d**
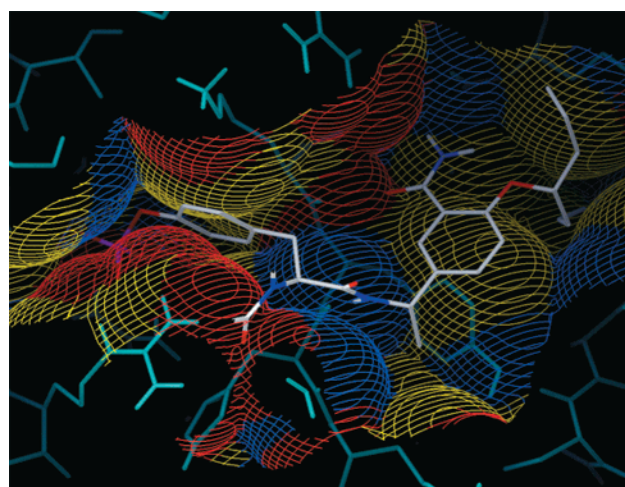

Figure 4. Predicted binding mode of compound **1f** (white) in Src SH2. The color designations for the solvent accessible surface of the protein are as follows: blue = H-bond acceptor groups; red = H-bond donor groups; yellow = hydrophobic groups.[27]

and **1e** draw attention to a common structural feature, which is the α-carbon branch point in the isopropyl and cyclohexyl R1 groups. The significance of this common feature becomes apparent in the bis-allyl compound **1f**, which binds over 2-fold better than **1a**. Inspection of the docked structure of compound **1f** in our Src SH2 model reveals how the branch point allows one allyl side chain to hug the surface of the protein while the other is able to extend deeply into the pY+3 pocket as seen in Figure 4. Attempts to probe deeper into the pY+3 pocket, as with compound **1g**, failed to increase affinity. Interestingly, this is the first example in this series where an increase in carbon atoms did not produce a corresponding increase in binding affinity. In fact, compound **1g** has two more carbon atoms than compound **1f**, yet binds more than 7-fold worse. This further illustrates the importance of proper spatial orientation of hydrophobic functionality to achieve ideal binding. The morpholine group of compound **1h**, which was included to increase aqueous solubility, greatly reduces binding affinity. Presumably, this result reflects an incompatibility of the positively charged

morpholine group (assay pH 7.2) with the hydrophobic pY+3 binding pocket of the Src SH2 domain.

Conclusion

A multifaceted approach encompassing both solid-phase parallel synthesis and structure-based methods was used to explore the pY+3 interactions at the Src SH2 domain with a series of phosphorylated nonpeptides. The combination of solid- and solution-phase reaction schemes allowed us to rapidly produce compounds with the necessary complexity dictated by our modeling studies. Guided by the FLO docking program we were able to identify unique pY+3 substituents (from commercially available sources), as in compound **1f**, which have provided insight as to the three-dimensional hydrophobic requirements of the pY+3 pocket for nonpeptide molecules. Furthermore, we demonstrated the flexibility of our solid-phase method by generating analogues of compound **2** that are void of any amino acid character. Such structure-based chemistry methodologies may be further exploited to design and generate future libraries of novel Src SH2 inhibitors, with the incorporation of additional diversity sites (e.g., pY+3, N-Ac, and p-Tyr mimics) to address cell potency and selectivity.

Experimental Section

General. Rink amide AM resin (0.66 mmol/g, 1% DVB, 200−400 mesh) and HOBt·H$_2$O (*N*-hydroxybenzotriazole monohydrate) were purchased from Calbiochem-Novabiochem Co. EDC (1-[3-dimethylaminopropyl]-3-ethyl-carbodiimide hydrochloride) was purchased from Advanced ChemTech. All other reagents and all Sure/Seal solvents (THF, DMF, CH$_2$Cl$_2$) were purchased from Aldrich Chemical Co. All solvents unless otherwise specified were HPLC grade and purchased from VWR Scientific Products. Unless otherwise specified, all solid-phase reactions were performed on a Nautilus 2400 organic synthesizer[20] with all reagents and solvents delivered to the reaction vessels via Ar through the closed fluid delivery system of the instrument. Melting points were determined using a Fisher-Johns melting point apparatus and are uncorrected. Analytical HPLC analysis was performed on a Hewlett-Packard series 1050 using a Vydac C18 column (3 μm, 4.6 × 100 mm, 2.0 mL/min flow rate) in a CH$_3$CN/H$_2$O (0.1% TFA) solvent system with a linear gradient of 10.7%/min from 10 to 90% CH$_3$CN. Millipore Ultrafree-MC centrifugal 0.45 μm filter units were used to prepare analytical samples for solid-phase reaction assessment. HPLC percent purities were assessed using peak area integration at 220 nm. RP-HPLC semipreparative purification was performed on a Rainin Dynamax purification system using a Vydac C18 column (10−15 μm, 50 × 250 mm, 50.0 mL/min flow rate) in a CH$_3$CN/H$_2$O (0.1% TFA) solvent system. LRMS spectra were obtained on a Micromass Platform II quadrupole mass spectrometer operating in electrospray mode. NMR spectra were obtained on a Bruker ARX 300 spectrometer under the following conditions: ^{1}H NMR spectra were recorded at 300.1 MHz using DMSO-d_6 (δ 2.50) as an internal standard; ^{31}P NMR spectra were recorded at 121.5 MHz using an external phosphoric acid standard (δ 0.0); ^{19}F NMR spectra were recorded at 282.4

MHz using an external trifluoroacetic acid standard (δ 0.0). ^{1}H NMR peak assignments were made using 2D COSY experiments. Interpretation of the ^{1}H NMR spectra for the final products (~50:50 diastereomeric mixture) reflects a combined proton count for both diastereomers and does not attempt to associate a particular shift with a particular diastereomer nor relative shifts for individual diastereomers. High-resolution mass spectral analyses were performed by Andrew Tyler (Harvard University Mass Spectrometry Laboratory). CONCORD was utilized according to *CONCORD User's Manual* (by Pearlman, R. S.), distributed by Tripos Inc., St. Louis, MO.

5-(1-Amino-ethyl)-2-hydroxy-benzoic Acid Methyl Ester Hydrochloride (5). A solution of methyl 5-acetyl-salicylate (5.0 g, 0.026 mol) and hydroxylamine hydrochloride (2.68 g, 0.039 mol) in 90 mL of pyridine was stirred at ambient temperature for 22 h. The reaction solution was concentrated on a rotary evaporator (55 °C), diluted with EtOAc (700 mL), and washed successively with 5% citric acid (3 × 250 mL) and brine (1 × 250 mL). The organic layer was dried over MgSO$_4$ and concentrated to afford the crude oxime product, which was subsequently used without purification in the next step: ^{1}H NMR (DMSO-d_6) δ 11.10 (s, 1H, O*H*), 10.55 (s, 1H, O*H*), 8.03 (d, *J* = 2.2 Hz, 1H, Ar*H*), 7.81 (dd, *J* = 8.7, 2.2 Hz, 1H, Ar*H*), 7.00 (d, *J* = 8.7 Hz, 1H, Ar*H*), 3.90 (s, 3H, CO$_2$C*H*$_3$), 2.12 (s, 3H, C*H*$_3$).

A mixture of the crude oxime (0.026 mol) and wet Raney nickel (2.2 g, 40 wt %/wt) in 130 mL of 5:1 EtOH (absolute)/Et$_3$N was hydrogenated using a Parr apparatus (45−50 psi) for 23 h. The reaction mixture was filtered through Celite, the Celite washed with ethanol, and the filtrate concentrated and resubjected to the above hydrogenation conditions (~50 psi) for 15 h. Isolation of the crude product as described above provided a light green oil, which was purified by flash chromatography (30:1, CH$_2$Cl$_2$/MeOH then 10:1, CH$_2$Cl$_2$/MeOH) to provide a yellow oil. Formation of the amine hydrochloride through trituration with ~50 mL of HCl·Et$_2$O (1.0 M) followed by filtration and removal of the excess solvent in vacuo (desiccator) provided 4.47 g (75%, 2 steps) of **2** as a white powder: mp 168−169 °C; ^{1}H NMR (DMSO-d_6) δ 10.54 (s, 1H, O*H*), 8.45 (br s, 3H, N*H*$_3$$^+$), 7.92 (d, *J* = 2.3 Hz, 1H, Ar*H*), 7.68 (dd, *J* = 8.6, 2.3 Hz, 1H, Ar*H*), 7.05 (d, *J* = 8.6 Hz, 1H, Ar*H*), 4.39 (m, 1H, C*H*Ph), 3.91 (s, 3H, CO$_2$C*H*$_3$), 1.49 (d, *J* = 6.8 Hz, 3H, C*H*$_3$CHPh).

5-(1-Allyloxycarbonylamino-ethyl)-2-hydroxy-benzoic Acid (6). To a suspension of amine hydrochloride **5** (3.0 g, 0.013 mol) in 23 mL of DME (ethylene glycol dimethyl ether) was added 22.5 mL (0.052 mol) of 2.3 N NaOH, and the resulting colorless solution stirred at ambient temperature for 19 h. After observing the complete absence of the starting methyl ester peak by HPLC, the reaction solution was diluted with 15 mL of H$_2$O and 20 mL of DME, followed by the addition of a solution of diallyl pyrocarbonate (5.3 g, 0.028 mol) in 10 mL of DME. The resulting white suspension (immediate ppt) was stirred at ambient temperature for 27 h. The reaction mixture was partitioned between 50:50 H$_2$O/EtOAc (600 mL), the layers separated, and the aqueous layer further extracted with EtOAc (2 × 150 mL). Upon acidification of the aqueous layer to pH = 1−2 with concentrated

HCl at 0 °C, the aqueous layer was extracted with EtOAc (3 × 150 mL) and the combined organic layers washed with brine, dried over MgSO$_4$, and concentrated to provide the crude product. Recrystallization from EtOAc/CH$_2$Cl$_2$ provided 3.13 g (91%, 2 steps) of the salicylic acid template **6** as a pinkish-white solid: mp 122−125 °C; ^{1}H NMR (DMSO-d_6) δ 11.00 (br s, 1H), 7.73 (m, 2H), 7.44 (dd, J = 8.5, 2.2 Hz, 1H, Ar*H*), 6.89 (d, J = 8.5 Hz, 1H, Ar*H*), 5.87 (m, 1H, C*H*=CH$_2$), 5.26 (d, J = 17.4, 1H, CH=CH*H* trans), 5.15 (d, J = 10.3, 1H, −CH=CH*H* cis), 4.61 (m, 1H, C*H*Ph), 4.43 (m, 2H, OC*H*$_2$), 1.31 (d, J = 7.0 Hz, 3H, C*H$_3$*CHPh); m/z 264 (M − H).

Batch Preparation of Salicylamide Resin (7). To a 250 mL Erlenmeyer flask containing 6.0 g (0.66 mmol/g, 3.96 mmol) of Rink amide AM resin was added 120 mL of 20% piperidine/DMA, and the resin mixture was rotated on an orbital shaker at ambient temperature for 20 min. The resin was then filtered (vacuum) via a Büchner funnel (pre-silylated using 5% SurfaSil in hexanes; Pierce Chemical Company), and the resin washed successively with DMA (5 × 60 mL) and CH$_2$Cl$_2$ (3 × 60 mL). The washed resin was then transferred to a 250 mL Erlenmeyer flask (pre-silylated) containing 2.3 g (0.012 mol) of EDC and 1.8 g (0.012 mol) of HOBt·H$_2$O, and to this was added a solution of salicylic acid template **6** (3.1 g, 0.012 mol) in 120 mL of 3:1 CH$_2$Cl$_2$/DMA. The resin mixture was rotated on an orbital shaker at ambient temperature for 17 h. The resin was then filtered as above and washed successively with DMA (5 × 60 mL), CH$_2$Cl$_2$ (5 × 60 mL), Et$_2$O (2 × 60 mL), CH$_2$Cl$_2$ (1 × 60 mL), Et$_2$O (1 × 60 mL), and CH$_2$Cl$_2$ (2 × 60 mL). Excess solvent was removed in vacuo overnight (desiccator) to provide 5.9 g of the derivatized resin **7** (assumed a theoretical loading capacity of 0.65 mmol/g based on 100% conversion). A resin aliquot of **7** (20 mg) was cleaved with 5% TFA/CH$_2$Cl$_2$ (~5 min), as described in the text, to provide analytical data: 99−100% HPLC purity; ^{1}H NMR (DMSO-d_6) δ 12.75 (br s, 1H), 8.31 (br s, 1H), 7.77 (br s, 2H), 7.59 (br d, 1H), 7.37 (d, J = 8.5 Hz, 1H, Ar*H*), 6.84 (d, J = 8.5 Hz, 1H, Ar*H*), 5.88 (m, 1H, C*H*=CH$_2$), 5.26 (d, J = 17.0, 1H, CH=CH*H* trans), 5.15 (d, J = 10.1, 1H, CH=CH*H* cis), 4.59 (m, 1H, C*H*Ph), 4.45 (s, 2H, OC*H*$_2$), 1.33 (d, J = 6.9 Hz, 3H, C*H$_3$*CHPh); m/z 263 (M − H).

General Mitsunobu Procedure for the Preparation of Ether Resin (8). To a pre-silylated RV (reaction vessel) containing 0.2 g (0.65 mmol/g theoretical, 0.13 mmol) of resin **7** was added 3.0 mL of THF (anhydrous), the resin was mixed for several minutes, and the RV was drained. To the swelled resin was added successively 1.0 mL (0.65 mmol) of a 0.65 M solution of triphenylphosphine in THF, 0.5 mL (0.65 mmol) of a 1.3 M solution of {R}-OH alcohol in THF (+ 0.7 mL THF chase), and 1.0 mL (0.65 mmol) of a 0.65 M solution of diethyl azodicarboxylate in THF. The resin mixture was agitated for 6 h, upon which the RV was drained and the resin washed successively with DMA (5 × 3.0 mL), CH$_2$Cl$_2$ (5 × 3.0 mL), Et$_2$O (2 × 3.0 mL), CH$_2$Cl$_2$ (1 × 3.0 mL), Et$_2$O (1 × 3.0 mL), and CH$_2$Cl$_2$ (2 × 3.0 mL). The above procedure was repeated (resin mixture agitated for 10 h) and the excess solvent removed in vacuo overnight

(desiccator) to provide the ether resin **8**. The following analytical data was obtained upon cleavage of **8a** (3−5 mg) with 30% TFA/CH$_2$Cl$_2$ (~5 min), as described in the text: 87% HPLC purity; m/z 279 (M + H).

General Amide Coupling Procedure for the Preparation of Phosphotyrosine Resin (9). To the dried resin **8** (0.13 mmol) was added 0.045 g (0.039 mmol) of tetrakis-(triphenylphosphine)palladium(0) followed by 4.0 mL of a 2:1 CH$_2$Cl$_2$/DMF degassed solution (degassed by bubbling Ar through the solution on the Nautilus 2400 instrument) containing triphenylphosphine (0.078 mmol, 0.02 M) and HOBt·H$_2$O (0.91 mmol, 0.23 M). The resin mixture was agitated for 3.5 h (top of instrument covered to exclude light), upon which the RV was drained and the resin washed successively with CH$_2$Cl$_2$ (5 × 3.0 mL), DMA (5 × 3.0 mL), CH$_2$Cl$_2$ (2 × 3.0 mL), Et$_2$O (2 × 3.0 mL), CH$_2$Cl$_2$ (1 × 3.0 mL), Et$_2$O (1 × 3.0 mL), and CH$_2$Cl$_2$ (2 × 3.0 mL) to provide the deprotected, slightly yellow resin. Resin aliquots (3−5 mg) were cleaved with 30% TFA/CH$_2$Cl$_2$ (~5 min), as described in the text, to verify complete deprotection (absence of Alloc-protected peak) by HPLC.

To the cooled (0 °C) CH$_2$Cl$_2$-swelled resin (0.13 mmol) was added 2.0 mL of a 2:1 CH$_2$Cl$_2$/DMA solution (pre-activated at 0 °C for 10 min) containing EDC (0.26 mmol, 0.13 M), HOBt·H$_2$O (0.26 mmol, 0.13 M), and R2-CO$_2$H (0.26 mmol, 0.13 M) followed by 1.0 mL (0.33 mmol) of a 0.33 M solution of *N,N*-diisopropylethylamine in 2:1 CH$_2$-Cl$_2$/DMA. The resin mixture was agitated at 0 °C for 1.5 h,[28] upon which the RV was drained and the resin washed (ambient temperature) successively with DMA (5 × 3.0 mL), CH$_2$Cl$_2$ (5 × 3.0 mL), Et$_2$O (2 × 3.0 mL), CH$_2$Cl$_2$ (1 × 3.0 mL), Et$_2$O (1 × 3.0 mL), and CH$_2$Cl$_2$ (2 × 3.0 mL) to provide the amide coupled resin **9**.

General Deprotection/Cleavage Procedure for the Generation of Phosphotyrosine Analogues (1 and 2). To the protected resin **9** (0.13 mmol) was added 3.0 mL of 95% TFA/2.5% H$_2$O/2.5% TIS (triisopropyl silane). After 2 h (periodic agitation) the filtrate was collected and the resin washed with CH$_2$Cl$_2$ (3 × 6.0 mL). The combined filtrates were concentrated, dissolved in DMSO (1.0 mL), and diluted with 50:50 CH$_3$CN/H$_2$O (3.0 mL) upon which the solution was filtered (0.2 μm, PTFE filter) and purified by RP-HPLC.

Phosphoric Acid Mono-(4-{(*S*)-2-acetylamino-2-[1-(3-carbamoyl-4-cyclohexylmethoxy-phenyl)-ethylcarbamoyl]-ethyl}-phenyl) Ester (1a). RP-HPLC purification (eluted at 55% CH$_3$CN) and lyophilization provided 0.031 g (43%) of **1a** as a white solid: mp 173−175 °C; ^{1}H NMR (DMSO-d_6; ~50:50 diastereomeric mixture) δ 8.45 (d, J = 7.7 Hz, 1H, CHCON*H*), 8.35 (d, J = 8.5 Hz, 1H, CHCON*H*), 8.02 (d, J = 8.3 Hz, 2 × 1H, Ac-N*H*), 7.77 (s, 2 × 1H, Ar*H*), 7.53 (m, 4H), 7.37−6.93 (m, 12H, Ar), 4.85 (m, 2 × 1H, C*H*Ph), 4.49 (m, 2 × 1H, C*H*CO[pTyr]), 3.92 (s, 2 × 2H, PhOC*H*$_2$), 2.87−2.61 (m, 2 × 2H, C*H*$_2$[pTyr]), 1.81−0.90 (m, 34H); ^{31}P NMR (DMSO) δ −0.943. HRMS calcd for C$_{27}$H$_{37}$N$_3$O$_8$P (M + H)$^+$: 562.2318. Found: 562.2301.

Phosphoric Acid Mono-(4-{(*S*)-2-acetylamino-2-[1-(3-carbamoyl-4-methoxy-phenyl)-ethylcarbamoyl]-ethyl}-phenyl) Ester (1b). RP-HPLC purification (eluted at 35% CH$_3$CN) and lyophilization provided 0.029 g (47%) of **1b**

as a white solid: mp 186−188 °C; ^{1}H NMR (DMSO-d_6; ~50:50 diastereomeric mixture) δ 8.45 (d, J = 7.9 Hz, 1H, CHCON*H*), 8.34 (d, J = 8.2 Hz, 1H, CHCON*H*), 8.02 (d, J = 8.4 Hz, 2 × 1H, Ac-N*H*), 7.77 (s, 2 × 1H, Ar*H*), 7.61 (br s, 2H), 7.48 (br s, 2H), 7.38 (dd, J = 8.5, 2.4 Hz, 1H, Ar*H*), 7.23−7.00 (m, 11H, Ar), 4.86 (m, 2 × 1H, C*H*Ph), 4.51 (m, 2 × 1H, C*H*CO[pTyr]), 3.88 (s, 3H, PhOC*H₃*), 3.87 (s, 3H, PhOC*H₃*), 2.92−2.62 (m, 2 × 2H, C*H₂*[pTyr]), 1.77 (s, 3H, C*H₃*[Ac]), 1.76 (s, 3H, C*H₃*[Ac]), 1.33 (d, J = 7.0 Hz, 3H, C*H₃*CHPh), 1.23 (d, J = 6.9 Hz, 3H, C*H₃*CHPh); ^{31}P NMR (DMSO) δ −0.976. HRMS calcd for $C_{21}H_{27}N_3O_8P$ (M + H)$^+$: 480.1535. Found: 480.1560.

Phosphoric Acid Mono-(4-{(*S*)-2-acetylamino-2-[1-(3-carbamoyl-4-ethoxy-phenyl)-ethylcarbamoyl]-ethyl}-phenyl) Ester (1c). RP-HPLC purification (eluted at 38% CH₃CN) and lyophilization provided 0.045 g (70%) of **1c** as a white solid: mp 199−201 °C; ^{1}H NMR (DMSO-d_6; ~50:50 diastereomeric mixture) δ 8.45 (d, J = 7.9 Hz, 1H, CHCON*H*), 8.33 (d, J = 8.1 Hz, 1H, CHCON*H*), 8.02 (d, J = 8.3 Hz, 2 × 1H, Ac-N*H*), 7.79 (s, 2 × 1H, Ar*H*), 7.57 (br s, 2H), 7.51 (br s, 2H), 7.45−7.00 (m, 12H, Ar), 4.85 (m, 2 × 1H, C*H*Ph), 4.55−4.46 (m, 2 × 1H, C*H*CO[pTyr]), 4.20−4.12 (m, 2 × 2H, PhOC*H₂*), 2.92−2.62 (m, 2 × 2H, C*H₂*[Tyr]), 1.77 (s, 3H, C*H₃*[Ac]), 1.76 (s, 3H, C*H₃*[Ac]), 1.40−1.32 (m, 9H), 1.23 (d, J = 6.9 Hz, 3H, C*H₃*CHPh); ^{31}P NMR (DMSO) δ −0.964. HRMS calcd for $C_{22}H_{29}N_3O_8P$ (M + H)$^+$: 494.1692. Found: 494.1704.

Phosphoric Acid Mono-(4-{(*S*)-2-acetylamino-2-[1-(3-carbamoyl-4-isopropoxy-phenyl)-ethylcarbamoyl]-ethyl}-phenyl) Ester (1d). RP-HPLC purification (eluted at 42% CH₃CN) and lyophilization provided 0.050 g (76%) of **1d** as a white solid: mp 179−181 °C; ^{1}H NMR (DMSO-d_6; ~50:50 diastereomeric mixture) δ 8.45 (d, J = 7.7 Hz, 1H, CHCON*H*), 8.34 (d, J = 7.9 Hz, 1H, CHCON*H*), 8.19 (d, J = 7.7 Hz, 2 × 1H, Ac-N*H*), 7.80 (s, 2 × 1H, Ar*H*), 7.57 (br s, 2H), 7.51 (br s, 2H), 7.44−7.01 (m, 12H, Ar), 4.85 (m, 2 × 1H, C*H*Ph), 4.75 (m, 2 × 1H, PhOC*H*), 4.49 (m, 2 × 1H, C*H*CO[pTyr]), 2.90−2.62 (m, 2 × 2H, C*H₂*[Tyr]), 1.77 (s, 3H, C*H₃*[Ac]), 1.76 (s, 3H, C*H₃*[Ac]), 1.32 (m, 15H), 1.23 (d, J = 6.8 Hz, 3H, C*H₃*CHPh); ^{31}P NMR (DMSO) δ −0.962. HRMS calcd for $C_{23}H_{31}N_3O_8P$ (M + H)$^+$: 508.1849. Found: 508.1844.

Phosphoric Acid Mono-(4-{(*S*)-2-acetylamino-2-[1-(3-carbamoyl-4-cyclohexyloxy-phenyl)-ethylcarbamoyl]-ethyl}-phenyl) Ester (1e). RP-HPLC purification (eluted at 51% CH₃CN) and lyophilization provided 0.041 g (58%) of **1e** as a white solid: mp 184−186 °C; ^{1}H NMR (DMSO-d_6; ~50:50 diastereomeric mixture) δ 8.46 (d, J = 7.9 Hz, 1H, CHCON*H*), 8.34 (d, J = 8.2 Hz, 1H, CHCON*H*), 8.02 (d, J = 8.3 Hz, 2 × 1H, Ac-N*H*), 7.81 (m, 2 × 1H, Ar*H*), 7.57 (m, 4H), 7.36−7.01 (m, 12H, Ar), 4.86 (m, 2 × 1H, C*H*Ph), 4.54 (m, 4H), 2.90−2.62 (m, 2 × 2H, C*H₂*[Tyr]), 1.93 (m, 2 × 2H, C*H₂*), 1.77 (s, 3H, C*H₃*[Ac]), 1.76 (s, 3H, C*H₃*[Ac]), 1.66−1.22 (m, 22H); ^{31}P NMR (DMSO) δ −0.961. HRMS calcd for $C_{26}H_{35}N_3O_8P$ (M + H)$^+$: 548.2162. Found: 548.2170.

Phosphoric Acid Mono-[4-((*S*)-2-acetylamino-2-{1-[4-(1-allyl-but-3-enyloxy)-3-carbamoyl-phenyl]-ethylcarbamoyl}-ethyl)-phenyl] Ester (1f). RP-HPLC purification

(eluted at 52% CH₃CN) and lyophilization provided 0.023 g (32%) of **1f** as a white solid: mp 180−182 °C; ^{1}H NMR (DMSO-d_6; ~50:50 diastereomeric mixture) δ 8.46 (d, J = 8.5 Hz, 1H, CHCON*H*), 8.35 (d, J = 8.3 Hz, 1H, CHCON*H*), 8.02 (d, J = 8.2 Hz, 2 × 1H, Ac-N*H*), 7.81 (s, 2 × 1H, Ar*H*), 7.52 (s, 2H), 7.48 (s, 2H), 7.37−7.01 (m, 12H, Ar), 5.86 (m, 2 × 2H, bis C*H*=CH₂), 5.15−5.07 (m, 2 × 4H, bis CH=C*H₂*), 4.85 (m, 2 × 1H, C*H*Ph), 4.70 (m, 2 × 1H, PhOC*H*), 4.51 (m, 2 × 1H, C*H*CO[pTyr]), 2.90−2.62 (m, 2 × 2H, C*H₂*[Tyr]), 2.45 (m, 2 × 4H, bis C*H₂*CH=CH₂), 1.77 (s, 3H, C*H₃*[Ac]), 1.76 (s, 3H, C*H₃*[Ac]), 1.34 (d, J = 6.8 Hz, 3H, C*H₃*CHPh), 1.23 (d, J = 6.9 Hz, 3H, C*H₃*CHPh); ^{31}P NMR (DMSO) δ −0.959. HRMS calcd for $C_{27}H_{35}N_3O_8P$ (M + H)$^+$: 560.2162. Found: 560.2178.

Phosphoric Acid Mono-[4-((*S*)-2-acetylamino-2-{1-[3-carbamoyl-4-(3-phenyl-propoxy)-phenyl]-ethylcarbamoyl}-ethyl)-phenyl] Ester (1g). RP-HPLC purification (eluted at 55% CH₃CN) and lyophilization provided 0.045 g (59%) of **1g** as a white solid: mp 188−190 °C; ^{1}H NMR (DMSO-d_6; ~50:50 diastereomeric mixture) δ 8.45 (d, J = 7.9 Hz, 1H, CHCON*H*), 8.34 (d, J = 8.2 Hz, 1H, CHCON*H*), 8.02 (d, J = 8.5 Hz, 2 × 1H, Ac-N*H*), 7.77 (m, 2 × 1H, Ar*H*), 7.56 (br s, 4H), 7.37−7.00 (m, 22H, Ar), 4.86 (m, 2 × 1H, C*H*Ph), 4.50 (m, 2 × 1H, C*H*CO[pTyr]), 4.10 (m, 2 × 2H, PhOC*H₂*), 2.92−2.62 (m, 8H), 2.08 (m, 2 × 2H, C*H₂*CH₂Ph), 1.77 (s, 3H, C*H₃*[Ac]), 1.76 (s, 3H, C*H₃*[Ac]), 1.34 (d, J = 6.9 Hz, 3H, C*H₃*CHPh), 1.23 (d, J = 7.0 Hz, 3H, C*H₃*CHPh); ^{31}P NMR (DMSO) δ −0.962. HRMS calcd for $C_{29}H_{35}N_3O_8P$ (M + H)$^+$: 584.2162. Found: 584.2189.

Phosphoric Acid Mono-[4-((*S*)-2-acetylamino-2-{1-[3-carbamoyl-4-(2-morpholin-4-yl-ethoxy)-phenyl]-ethylcarbamoyl}-ethyl)-phenyl] Ester (1h). RP-HPLC purification (eluted at 20% CH₃CN) and lyophilization provided 0.056 g (62%) of **1h** as a white solid: mp 205−207 °C; ^{1}H NMR (DMSO-d_6; ~50:50 diastereomeric mixture) δ 8.38 (m, 2 × 1H, CHCON*H*), 8.06 (d, J = 8.1 Hz, 2 × 1H, Ac-N*H*), 7.84−6.92 (m, 18H, Ar*H*), 4.85 (m, 2 × 1H, C*H*Ph), 4.48 (m, 6H), 3.86 (br s, 2 × 4H, morph), 3.52 (br s, 2 × 2H, PhOCH₂C*H₂*), 3.30 (br s, 2 × 4H, morph), 2.91−2.64 (m, 2 × 2H, C*H₂*[Tyr]), 1.81 (d, J = 1.8 Hz, 3H, C*H₃*[Ac]), 1.76 (d, J = 2.0 Hz, 3H, C*H₃*[Ac]), 1.30 (d, J = 5.7 Hz, 3H, C*H₃*CHPh), 1.24 (d, J = 5.9 Hz, 3H, C*H₃*CHPh); ^{31}P NMR (DMSO-d_6) δ −0.852, −0.924; ^{19}F NMR (DMSO-d_6) δ −69.79. HRMS calcd for $C_{26}H_{36}N_4O_9P$ (M + H)$^+$: 579.2220. Found: 579.2225.

Phosphoric Acid Mono-{4-[1-(3-carbamoyl-4-cyclohexylmethoxy-phenyl)-ethylcarbamoyl]-phenyl} Ester (2a). RP-HPLC purification (eluted at 49% CH₃CN) and lyophilization provided 0.024 g (39%) of **2a** as a white solid: mp 165−167 °C; ^{1}H NMR (DMSO-d_6) δ 8.74 (d, J = 7.9 Hz, 1H, CON*H*), 7.88−7.06 (m, 9H), 5.12 (m, 1H, C*H*Ph), 3.92 (d, J = 5.5 Hz, 2H, PhOC*H₂*), 1.81−1.69 (m, 6H, Chx), 1.45 (d, J = 6.8 Hz, 3H, C*H₃*CHPh), 1.27−1.03 (m, 5H, Chx); ^{31}P NMR (DMSO-d_6) δ −1.28. HRMS calcd for $C_{23}H_{29}N_2O_7P$ (M−H)$^-$: 475.1634. Found: 475.1616.

Phosphoric Acid Mono-{4-[1-(3-carbamoyl-4-isopropoxy-phenyl)-ethylcarbamoyl]-phenyl} Ester (2d). RP-HPLC purification (eluted at 35% CH₃CN) and lyophilization provided 0.027 g (50%) of **2d** as a white solid: mp 164−

166 °C; ^{1}H NMR (DMSO-d_6) δ 8.74 (d, J = 7.8 Hz, 1H, CON*H*), 7.89−7.09 (m, 9H), 5.12 (m, 1H, C*H*Ph), 4.74 (m, 1H, PhOC*H*), 1.46 (d, J = 6.9 Hz, 3H, C*H*$_3$CHPh), 1.32 [d, J = 5.9 Hz, 6H, (C*H*$_3$)$_2$CHO]; ^{31}P NMR (DMSO-d_6) δ −1.28. HRMS calcd for C$_{19}$H$_{23}$N$_2$O$_7$P (M − H)$^-$: 421.1165. Found: 421.1147.

Phosphoric Acid Mono-(4-{1-[4-(1-allyl-but-3-enyloxy)-3-carbamoyl-phenyl]-ethylcarbamoyl}-phenyl) Ester (2f). RP-HPLC purification (eluted at 46% CH$_3$CN) and lyophilization provided 0.014 g (23%) of **2f** as a white solid: mp 152−154 °C; ^{1}H NMR (DMSO-d_6) δ 8.74 (d, J = 7.9 Hz, 1H, CON*H*), 7.89−7.13 (m, 9H), 5.93−5.79 (m, 2 × 1H, bis C*H*=CH$_2$), 5.35−4.91 (m, 5H), 4.68 (m, 1H, PhOC*H*), 2.46 (m, 4H), 1.46 (d, J = 6.8 Hz, 3H, C*H*$_3$CHPh); ^{31}P NMR (DMSO-d_6) δ −1.26. HRMS calcd for C$_{23}$H$_{27}$N$_2$O$_7$P (M − H)$^-$: 473.1478. Found: 473.1496.

Phosphoric Acid Mono-(4-{1-[3-carbamoyl-4-(3-phenyl-propoxy)-phenyl]-ethylcarbamoyl}-phenyl) Ester (2g). RP-HPLC purification (eluted at 48% CH$_3$CN) and lyophilization provided 0.025 g (39%) of **2g** as a white solid: mp 159−161 °C; ^{1}H NMR (DMSO-d_6) δ 8.74 (d, J = 7.6 Hz, 1H, CON*H*), 7.89−7.04 (m, 14H), 5.13 (m, 1H, C*H*Ph), 4.09 (m, 2H, PhOC*H*$_2$), 2.74 (m, 2H, CH$_2$C*H*$_2$Ph), 2.08 (m, 2H, C*H*$_2$CH$_2$Ph), 1.46 (d, J = 6.7 Hz, 3H, C*H*$_3$CHPh); ^{31}P NMR (DMSO-d_6) δ −1.28. HRMS calcd for C$_{25}$H$_{27}$N$_2$O$_7$P (M − H)$^-$: 497.1478. Found: 497.1457.

References and Notes

(1) (a) Chang, Y.-T.; Gray, N. S.; Rosania, G. R.; Sutherlin, D. P.; Kwon, S.; Norman, T. C.; Sarohia, R.; Leost, M.; Meijer, L.; Schultz, P. G. *Chem. Biol.* **1999**, *6*, 361−375. (b) Rohrer, S. P.; Birzin, E. T.; Mosley, R. T.; Berk, S. C.; Hutchins, S. M.; Shen, D.-M.; Xiong, Y.; Hayes, E. C.; Parmar, R. M.; Foor, F.; Mitra, S. W.; Degrado, S. J.; Shu, M.; Klopp, J. M.; Cai, S.-J.; Blake, A.; Chan, W. W. S.; Pasternak, A.; Yang, L.; Patchett, A. A.; Smith, R. G.; Chapman, K. T.; Schaeffer, J. M. *Science* **1998**, *282*, 737−740. (c) Brady, S. F.; Stauffer, K. J.; Lumma, W. C.; Smith, G. M.; Ramjit, H. G.; Lewis, S. D.; Lucas, B. J.; Gardell, S. J.; Lyle, E. A.; Appleby, S. D.; Cook, J. J.; Holahan, M. A.; Stranieri, M. T.; Lynch Jr., J. J.; Lin, J. H.; Chen, I.-W.; Vastag, K.; Naylor-Olsen, A. M.; Vacca, J. P. *J. Med. Chem.* **1998**, *41*, 401−406. For recent reviews, see: (d) Fahad, O.-A.; Ostrem, J. A. *Drug Discovery Today* **1998**, *3*, 223−231. (e) Hoekstra, W. J.; Poulter, B. L. *Curr. Med. Chem.* **1998**, *5*, 195−204. (f) Fecik, R. A.; Frank, K. E.; Gentry, E. J.; Menon, S. R.; Mitscher, L. A.; Telikepalli, H. *Med. Res. Rev.* **1998**, *18*, 149−185. (g) Dolle, R. E. *Mol. Diversity* **1997**, *2*, 223−236. (h) Lam, K. S. *Anti-Cancer Drug Des.* **1997**, *12*, 145−167. (i) Balkenhohl, F.; Bussche-Hünnefeld, C. von dem; Lansky, A.; Zechel, C. *Angew. Chem., Int. Ed. Engl.* **1996**, *35*, 2288−2337. (j) Ellman, J. A. *Acc. Chem. Res.* **1996**, *29*, 132−143.

(2) Such a strategy utilizes the philosophy of "resin capture," as introduced by Armstrong and Keating: Keating, T. A.; Armstrong, R. W. *J. Am. Chem. Soc.* **1996**, *118*, 2574−2583. See also: Brown, S. D.; Armstrong, R. W. *J. Am. Chem. Soc.* **1996**, *118*, 6331−6332.

(3) For examples of structure-based methods used in combinatorial chemistry, see: (a) Antel, J. *Curr. Opin. Drug Discovery Dev.* **1999**, *2*, 224−233. (b) Szardenings, K. A.; Harris, D.; Lam, S.; Shi, L.; Tien, D.; Wang, Y.; Patel, D. V.; Navre, M.; Campbell, D. A. *J. Med. Chem.* **1998**, *41*, 2194−2200. (c) Kick, E. K.; Roe, D. C.;

Skillman, A. G.; Liu, G.; Ewing, T. J. A.; Sun, Y.; Kuntz, I. D.; Ellman, J. A. *Chem. Biol.* **1997**, *4*, 297−307. (d) Combs, A. P.; Kapoor, T. M.; Feng, S.; Chen, J. K.; Daude-Snow, L. F.; Schreiber, S. L. *J. Am. Chem. Soc.* **1996**, *118*, 287−288.

(4) Songyang, Z.; Shoelson, S. E.; Chaudhuri, M.; Gish, G.; Pawson, T.; Haser, W. G.; King, F.; Roberts, T.; Ratnofsky, S.; Lechleider, R. J.; Neel, B. G.; Birge, R. B.; Fajardo, J. E.; Chou, M. M.; Hanafusa, H.; Schaffhausen, B.; Cantley, L. C. *Cell* **1993**, *72*, 767−778.

(5) Pawson, T. *Nature* **1995**, *373*, 573−580.

(6) Cohen, G. B.; Ren, R.; Baltimore, D. *Cell* **1995**, *80*, 237−248.

(7) Botfield, M. C.; Green, J. *Ann. Rep. Med. Chem.* **1995**, *30*, 227−237.

(8) Brugge, J. S. *Science* **1993**, *260*, 918−919.

(9) Saltiel, A. R.; Sawyer, T. K. *Chem. Biol.* **1996**, *3*, 887−893.

(10) Waksman, G.; Kominos, D.; Robertson, S. R.; Pant, N.; Baltimore, D.; Birge, R. B.; Cowburn, D.; Hanafusa, H.; Mayer, B. J.; Overduin, M.; Resh, M. D.; Rios, C. B.; Silverman, L.; Kuriyan, J. *Nature* **1992**, *358*, 646−653.

(11) Waksman, G.; Shoelson, S. E.; Pant, N.; Cowburn, D.; Kuriyan, J. *Cell* **1993**, *72*, 779−790.

(12) Bibbins, K. B.; Boeuf, H.; Varmus, H. E. *Mol. Cell. Biol.* **1993**, *13*, 7278−7287.

(13) For a recent review, see: (a) Sawyer, T. K. *Biopolymers (Pept. Sci.)* **1998**, *47*, 243−261. Also, see: (b) Lee, R. T.; Lawrence, D. S. *J. Med. Chem.* **1999**, *42*, 784−787. (c) Llinas-Brunet, M.; Beaulieu, P. L.; Cameron, D. R.; Ferland, J.-M.; Gauthier, J.; Ghiro, E.; Gillard, J.; Gorys, V.; Poirier, M.; Rancourt, J.; Wernic, D.; Betageri, R.; Cardozo, M.; Jakes, S.; Lukas, S.; Patel, U.; Proudfoot, J.; Moss, N. *J. Med. Chem.* **1999**, *42*, 722−729. (d) Schoepfer, J.; Fretz, H.; Gay, B.; Furet, P.; Garcia-Echeverria, C.; End, N.; Caravatti, G. *Bioorg. Med. Chem. Lett.* **1999**, *9*, 221−226. (e) Alligood, K. J.; Charifson, P. S.; Crosby, R.; Consler, T. G.; Feldman, P. L.; Gampe, R. T., Jr.; Gilmer, T. M.; Jordan, S. R.; Milstead, M. W.; Mohr, C.; Peel, M. R.; Rocque, W.; Rodriguez, M.; Rusnak, D. W.; Shewchuk, L. M.; Sternbach, D. D. *Bioorg. Med. Chem. Lett.* **1998**, *8*, 1189−1194. (f) Charifson, P. S.; Shewchuk, L. M.; Rocque, W.; Hummel, C. W.; Jordan, S. R.; Mohr, C.; Pacofsky, G. L.; Peel, M. R.; Rodriguez, M.; Sternbach, D. D.; Consler, T. G. *Biochemistry* **1997**, *36*, 6283−6293. (g) Plummer, M. S.; Lunney, E. A.; Para, K. S.; Shahripour, A.; Stankovic, C. J.; Humblet, C.; Fergus, J. H.; Marks, J. S.; Herrera, R.; Hubbell, S.; Saltiel, A.; Sawyer, T. K. *Bioorg. Med. Chem.* **1997**, *5*, 41−47. (h) Plummer, M. S.; Lunney, E. A.; Para, K. S.; Vara Prasad, J. V. N.; Shahripour, A.; Singh, J.; Stankovic, C. J.; Humblet, C.; Fergus, J. H.; Marks, J. S.; Sawyer, T. K. *Drug Des. Discovery* **1996**, *13*, 75−81. (i) Rodriguez, M.; Crosby, R.; Alligood, K. J.; Gilmer, T. M.; Berman, J. *Lett. Pept. Sci.* **1995**, *2*, 1−6. (j) Gilmer, T. M.; Rodriguez, M.; Jordan, S.; Crosby, R.; Alligood, K. J.; Green, M.; Kimery, M.; Wagner, C.; Kinder, D.; Charifson, P.; Hassell, A. M.; Willard, D.; Luther, M.; Rusnak, D.; Sternbach, D. D.; Mehrotra, M.; Peel, M.; Shampine, L.; Davis, R.; Robbins, J.; Patel, I. R.; Kassel, D.; Burkhart, W.; Moyer, M.; Bradshaw, T.; Berman, J. *J. Biol. Chem.* **1994**, *269*, 31711−31719.

(14) (a) Violette, S. M.; Shakespeare, W. C.; Bartlett, C.; Guan, W.; Smith, J. A.; Rickles, R. J.; Bohacek, R. S.; Holt, D. A.; Baron, R.; Sawyer, T. K. *Chem. Biol.* **2000**, *7*, 225−235. (b) Luke, G. P. and Holt, D. A. *Tetrahedron: Asymmetry* **1999**, *10*, 4393−4403. (c) Buchanan, J. L.; Bohacek, R. S.; Luke, G. P.; Hatada, M. H.; Lu, X.; Dalgarno, D. C.; Narula, S. S.; Yuan, R.; Holt, D. A. *Bioorg. Med. Chem. Lett.* **1999**, *9*, 2353−2358. (d) Buchanan, J. L.; Vu, C. B.; Merry, T. J.; Corpuz, E. G.; Pradeepan, S. G.; Mani, U. N.; Yang, M.; Plake, H. R.; Varkhedkar, V. M.; Lynch, B. A.; MacNeil, I. A.; Loiacono, K. A.; Tiong, C. L.; and Holt, D. A. *Bioorg. Med. Chem. Lett.* **1999**, *9*, 2359−2364. (e) Metcalf, C. A., III; Vu, C. B.; Sundaramoorthi, R.; Jacobsen, V. A.; Laborde, E. A.; Green, J.; Green, Y.; Macek, K. J.; Merry, T. J.; Pradeepan, S. G.; Uesugi, M.; Varkhedkar, V. M.; Holt, D. A. *Tetrahedron Lett.* **1998**, *39*, 3435−3438.

(15) Plummer, M. S.; Holland, D. R.; Shahripour, A.; Lunney, E. A.; Fergus, J. H.; Marks, J. S.; McConnell, P.; Mueller, W. T.; Sawyer, T. K. *J. Med. Chem.* **1997**, *40*, 3719−3725.

(16) Lunney, E. A.; Para, K. S.; Rubin, J. R.; Humblet, C.; Fergus, J. H.; Marks, J. S.; Sawyer, T. K. *J. Am. Chem. Soc.* **1997**, *119*, 12471−12476.

(17) A recent X-ray structure (2.5 Å) of compound **1a** (higher affinity diastereomer) complexed with Lck SH2 (S162C) shows engagement of its cyclohexylmethyl group in the pY+3 domain of the protein (Bohacek, R. S.; Dalgarno, D. C.; Hatada, M.; Jacobsen, V. E.; Lynch,

B. A.; Macek, K. J.; Metcalf, C. A., III; Narula, S. S.; Violette, S. M.; Sawyer, T. K.; Weigele, M., submitted for publication). Therefore, modifications made to this end of the molecule are expected to interact with the pY+3 pocket.

(18) Lunney, E. A.; Para, K. S.; Plummer, M. S.; Prasad, J. V. N. V.; Saltiel, A. R.; Sawyer, T. K.; Shahripour, A.; Singh, J.; Stankovic, C. J. WO97/12903.

(19) Although we utilized the racemic salicylic template for our study, the chiral nonracemic (*S*)-amine (stereochemistry of higher affinity diastereomer) can be readily generated in 88−94% ee (ref 14b).

(20) Argonaut Technologies, San Carlos, CA.

(21) Silverberg, L. J.; Dillon, J. L.; Vemishetti, P. *Tetrahedron Lett.* **1996**, *37*, 771−774.

(22) Lynch, B. A.; Loiacono, K. A.; Tiong, C. L.; Adams, S. E.; MacNeil, I. A. *Anal. Biochem.* **1997**, *247*, 77−82.

(23) FLO97, Graphics and Molecular Mechanics Software for Drug Design. Available from Colin McMartin at Thistlesoft, e-mail: cmcma@ix.netcom.com.

(24) At the time we were designing molecules for this study, no high-resolution crystal structures of Src SH2 were available for docking studies. Therefore, the Lck SH2-peptide crystal structure was used not only because of the high quality (1.0 Å) of the structure but also because the binding site of Lck SH2 is almost identical to that of Src SH2 (for the X-ray structure, see: Tong, L.; Warren, T. C.; King, J.; Betageri, R.; Rose, J.; Jakes, S. *J. Mol. Biol.* **1996**, *256*, 601−610). We have had success using this model in the design of high-affinity inhibitors of Src SH2 and in the accurate prediction of their binding mode prior to determination by X-ray crystallography and NMR (see ref 14c and ref 17).

(25) McMartin, C.; Bohacek, R. S. *J. Comput.-Aided Mol. Des.* **1997**, *11*, 333−344.

(26) The literature IC_{50} value for **1a** is 1.0 μM (ref 18) as determined by an assay protocol measuring the competitive displacement of ^{35}S-labeled Src-SH2-GST from phosphorylated PDGF receptor kinase, as described in ref 13g. This value cannot be directly compared to our IC_{50} value due to differences in assay protocols, but nonetheless they are in the same range.

(27) Bohacek, R. S.; McMartin, C. *J. Med. Chem.* **1992**, *35*, 1671−84.

(28) For the synthesis of compound **2**, p-(OPO$_3$Bn$_2$)PhCO$_2$H was added at 0 °C upon which the resin mixture was stirred to ambient temperature overnight (14 h) and then processed as described.